Available online at www.sciencedirect.com

ScienceDirect

Procedia CIRP 133 (2025) 424–429

www.elsevier.com/locate/procedia

20th CIRP Conference on Modeling of Machining Operations

Mechanistic modeling of cutting forces in milling of unidirectional Glass Fiber Reinforced Polymer (UD-GFRP)

Matthias Nutte[a*], Edouard Rivière-Lorphèvre[a], Valentin Dambly[a], Pedro-José Arrazola[b], Ismail Lazoglu[c], Aurélie Granjon[d] , François Ducobu[a]

[a]*Machine Design and Production Engineering Lab, Research Institute for Science and Material Engineering, UMONS, Mons 7000, Belgium*
[b]*Mechanical and Manufacturing Department, Faculty of Engineering, Mondragon Unibertsitatea, Loramendi 4, Arrasate-Mondragón 20500, Spain*
[c]*Manufacturing and Automation Research Center, Koc University, Istanbul 34450, Turkey*
[d]*Sobelcomp SPRL. Rue de l'économie 13, 4431 Loncin, Belgium*

* Corresponding author. *E-mail address:* matthias.nutte@umons.ac.be

Abstract

Mechanistic models, established on experimental data, are recognized for their precision and simplicity in implementation. In this context of milling, the modeling of cutting forces, specifically radial and tangential components, has been extensively explored for unidirectional carbon fiber-reinforced polymer (UD-CFRP) parts. These models account for the anisotropic nature of fiber-reinforced polymers (FRPs), with cutting coefficients that vary based on the instantaneous cutting angle. However, due to the inherent flexibility of these materials, primarily attributed to their low thickness, axial cutting forces must also be incorporated to accurately represent the phenomena occurring during the machining process. This study develops a model for calculating cutting forces in three spatial directions for UD-GFRPs (unidirectional Glass Fiber-reinforced polymers). Building on an existing model from the literature for UD-CFRP, this new version introduces several modifications. First, the model validated for CFRPs must be extended to GFRPs. Secondly, the model must be extended from two dimensions to three dimensions. Finally, to ensure that the model includes only the actual contributions of the trimming operation, machining tests will be performed using only the rolling teeth. The cutting coefficients are modelled as a periodic function with a fundamental period of π. A first-order Fourier series was chosen for this purpose. Fourier series parameters are identified from the milling forces measured during a set of slotting operations at three feed rates and four fiber orientations. While the average levels of cutting forces are accurately modelled for both slotting and shoulder milling (with 50% immersion in up milling), the modeling of force amplitudes still requires improvement.

Keywords: Mechanistic model; Milling; Robotic machining; Cutting forces; UD GFRP

1. Introduction

Fiber-reinforced polymers (FRPs) are gaining widespread adoption across various industrial sectors due to their excellent strength-to-weight ratio and mechanical properties. As a result, there is significant interest in studying the trimming of FRP components, particularly since composite molding processes often require subsequent finishing operations to achieve the precise dimensional tolerances. These finishing operations, which are typically performed manually, are crucial for ensuring the final part meets the desired specifications. To effectively simulate the trimming process, it is essential to develop an accurate and comprehensive cutting force calculation model in all three spatial directions.

There are four categories of models for calculating cutting forces in milling for unidirectional fiber-reinforced polymers (UD-FRPs): macro-mechanical, micro-mechanical, numerical, and mechanistic models. Macro-mechanical models treat the material as homogeneous, useful for optimizing cutting parameters and reducing cutting forces, but they don't account

10.1016/j.procir.2025.02.073

for microchip formation [1]. Micro-mechanical models detail the composite's fibers and matrix, providing a more accurate cutting process representation, though they require numerous parameters and detailed calibration, limiting their practical application [1]. Numerical models, mainly based on finite element methods (FEM) [2], [3] and less commonly on discrete element models (DEM) [4], save resources and offer a precise description of the cutting process, but are limited by computational power and finite element theory constraints [1]. Mechanistic models, being semi-empirical, are intuitive for optimizing cutting parameters and tool geometries [1]. However, they require extensive and time-consuming experiments to ensure accuracy and applicability. Once cutting coefficients are determined, calculation time is minimal, making them suitable for industrial applications.

Most mechanistic models in literature propose identifying cutting coefficients as functions of the instantaneous fiber cutting angle. These functions can be represented as a Fourier series [5], a sinusoidal function [6] or polynomial functions [7], [8]. However, some studies consider constant coefficient cutting while accounting for fiber distribution [9], [10]. Additionally, Karpat's model [6] considers instantaneous cutting forces and is therefore subject to issues such as runout, vibration, initial immersion angle, and noise. Conversely, Mullin [5] considers average forces to avoid these problems, similar to Altintas' approach for metals [11]. Finally, only the modelling of tangential and radial forces in the plane (2D) is considered in most studies.

In this paper, three dimensional forces are modelled. To achieve this, a mechanistic model is developed based on an existing model [5]. The cutting coefficients are defined as a Fourier series. Average cutting forces will be used to avoid considering problems such as runout, vibrations, initial immersion angle, etc. Machining tests will be conducted on a machining robot. Each cutting condition will be repeated, mitigating issues related to fiber distribution, variable sample thickness, inclusions in samples, and machining defects (delamination, fiber pull-out, etc.). The aim is to correctly predict the average levels of cutting forces.

After explaining the geometrical convention in section 2, section 3 introduces the mechanistic cutting force model. Section 4 develops the method for identifying cutting coefficients. Section 5 details the experimental setup, and section 6 presents the model results.

Nomenclature

$(.)^+$	pseudo-inverse of a matrix
$()_w$	weighted matrix
β	instantaneous fiber cutting angle [rad]
θ	fiber orientation angle [rad]
φ_{ex}	exit angle [rad]
φ_{st}	start angle [rad]
φ_p	pitch angle between flutes [rad]
$\varphi_j(t)$	angular immersion of the jth flute [rad]
a_p	axial depth of cut [mm]
a_e	radial depth of cut [mm]
$\boldsymbol{C}$	feed per tooth matrix [mm/th]
C_i, S_i	Fourier coefficients
C_{iw}, S_{iw}	weighted Fourier coefficients
$\boldsymbol{F}$	mean cutting forces vector for all feed per tooth [N]
$F_.$	mean force along x, y and z axis
$\boldsymbol{f}$	means cutting forces for a specific feed per tooth [N]
f_z	feed per tooth [mm/th]
h	instantaneous uncut chip thickness
K_{pc}	cutting coefficients [MPa]
K_{pe}	edge coefficients [N/mm]
M	order of the Fourier series
m	number of fiber orientations angle
n	number of feed per tooth
t, r, a	tangential, radial and axial direction
v_c	cutting speed [m/min]
$\boldsymbol{W}$	weighting force vector
Z	numbers of flutes

2. Geometrical convention

The geometrical convention used in this study follows the Altintas convention [11]. In Fig. 1, milling of a UD-FRP (Unidirectional Fiber-reinforced Polymer) composite is illustrated.

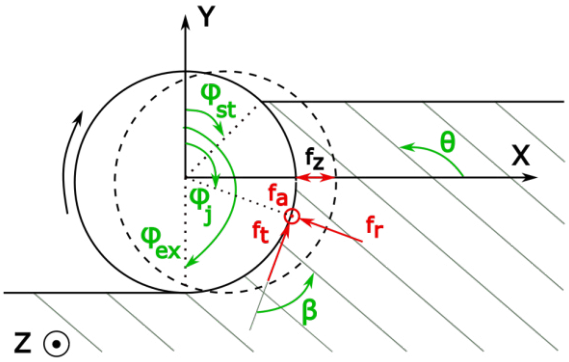

Fig. 1. Geometrical convention.

The XY reference frame is the frame perpendicular to the tool axis, with X as the feed direction and Y as the normal direction. The fiber direction angle, θ, is the angle between the X axis and the fibers, measured in the trigonometric direction. Tooth j is defined by its angle φ_j, measured from the Y axis in the anti-trigonometric direction. The tooth is engaged in the material between the start of immersion angle φ_{st} and the end of immersion angle φ_{ex}. The cutting force components (tangential t, radial r, and axial a) are applied at the tooth. The instantaneous fiber cutting angle, β, is the angle between the tangential direction and the fibers, measured in the trigonometric direction. For unidirectional cutting, β is related as follows (Eq. 1):

$$\beta(t) = \varphi_j(t) + \theta \tag{1}$$

3. Mechanistic cutting force model

Even though axial forces need to be limited in FRP machining to reduce the risk of delamination between plies, the tools designed by Seco Tools produce a reduced axial force [12]. These axial forces will nevertheless be modelled, along

with radial and tangential forces. The expression of the cutting force applied in radial, tangential and axial (Eq. 2) directions is similar to Altintas' model [13]

$$\begin{aligned} f_t(\phi_j) &= K_{tc}(\beta)a_p h(\phi_j) + K_{te}(\beta)a_p \\ f_r(\phi_j) &= K_{rc}(\beta)a_p h(\phi_j) + K_{re}(\beta)a_p \\ f_a(\phi_j) &= K_{ac}(\beta)a_p h(\phi_j) + K_{ae}(\beta)a_p \end{aligned} \quad (2)$$

Where a_p is the axial depth of cut, K_{tc}, K_{rc} and K_{ac} are cutting force coefficients in tangential, radial and axial directions, K_{te}, K_{re} and K_{ae} are edge force coefficients and h is the instantaneous uncut chip thickness which is function of the feed per tooth f_z and the angular immersion of the jth flute φ_j (Eq 3).

$$h(\varphi_j) = f_z \sin(\varphi_j) \quad (3)$$

The assumption adopted by Mullin et al [5] is that the cutting coefficients have a fundamental period of π. Given that the instantaneous fiber cutting angle β varies between 0 and π, and that the chip formation mechanism varies with β, the cutting coefficients have a fundamental period of π. It is therefore possible to express the cutting coefficients as follows (Eq 4):

$$K_{pq}(\beta) = \sum_{i=0}^{M} C_i^{pq} \cos(2i\beta) + S_i^{pq} \sin(2i\beta) \quad with\ p = \\ with\ p = t,r,a\ ;\ q = c,e \quad (4)$$

To have the simplest possible model with the least amount of testing, the order M of the Fourier series is set to the minimum possible (M=1). Moreover, this is the same order used by Mullin et al [5]. The use of a 2nd-order Fourier series would tend to give better results, thanks to the larger number of parameters. However, there is no physical reason for choosing a second order. The cutting coefficients therefore have the following form (Eq. 5):

$$K_{pq}(\beta) = C_0^{pq} + C_1^{pq} \cos(2\beta) + S_1^{pq} \sin(2\beta) \quad (5)$$

Section 4 will explain the method for identifying these cutting coefficients C_0^{pq}, C_1^{pq} and S_1^{pq}.

4. Identification method of the variable cutting coefficient

From the expression (Eq. 6) of the average cutting forces per tooth period expressed by Altintas [11], it is possible to determine the cutting coefficients.

$$F_q = \frac{1}{\varphi_p} \int_{\beta_{st}}^{\beta_{ex}} F_{q,inst}\, d\beta \ \ with\ q = x,y,z \quad (6)$$

The average cutting forces per tooth period F_x, F_y et F_z, depending respectively on the tool feed, normal to the feed, and out-of-plane, are the result of integrating the instantaneous forces $F_{x,inst}$, $F_{y,inst}$ and $F_{z,inst}$ while the tooth is in the immersion zone. The integral is divided by the pitch angle φ_p ($\varphi_p = 2\,\pi/Z$). The immersion zone of a tooth is defined as a function of the instantaneous fiber cutting angle (Eq. 7). This angle is the sum of the angular immersion of the jth flute φ_j and the fiber orientation angle θ. In the case of slotting, the start immersion angle φ_{st} is 0 and the exit immersion angle φ_{ex} is π.

$$\beta_{st} < \beta < \beta_{ex} \ \ with\ \beta(t) = \varphi_j(t) + \theta \quad (7)$$

The expressions for instantaneous forces are in Eq. 8 [11].

$$\begin{aligned} F_{x,inst}(\beta) &= \frac{f_z a_p}{2}(-K_{tc}(\beta)\sin(2\varphi) - K_{rc}(\beta)(1-\cos(2\varphi)) \\ &\quad + a_p(-K_{te}(\beta)\cos(2\varphi) - K_{re}(\beta)\sin(2\varphi)) \\ F_{y,inst}(\beta) &= \frac{f_z a_p}{2}(K_{tc}(\beta)(1-\cos(2\varphi) - K_{rc}(\beta)\sin(2\varphi)) \\ &\quad + a_p(K_{te}(\beta)\sin(2\varphi) - K_{re}(\beta)\cos(2\varphi)) \\ F_{z,inst}(\beta) &= f_z a_p K_{ac}(\beta)\sin(2\varphi) + a_p K_{ae}(\beta) \end{aligned} \quad (8)$$

Moreover, the average cutting forces can be expressed as a linear function of feed rate f_z and an offset contributed by the edge forces [11] (Eq. 9):

$$F_q = F_{qc}\, f_z + F_{qe} \ with\ q = x,y,z \quad (9)$$

On the other hand, it is possible to write the average forces in a vector $\boldsymbol{f}$ (Eq. 10):

$$\boldsymbol{f} = [F_x, F_y, F_z]^T \quad (10)$$

The average forces (Eq. 11) can be expressed in matrix form using the form:

$$\begin{aligned} \boldsymbol{f} &= \boldsymbol{c}\boldsymbol{b}(\theta)\ with\ \boldsymbol{c} = \begin{bmatrix} c & 1 & 0 & 0 & 0 & 0 \\ 0 & 0 & c & 1 & 0 & 0 \\ 0 & 0 & 0 & 0 & c & 1 \end{bmatrix} \\ \boldsymbol{b}(\theta) &= \begin{bmatrix} F_{xc} & F_{xe} & F_{yc} & F_{ye} & F_{zc} & F_{ze} \end{bmatrix}^T \end{aligned} \quad (11)$$

In addition, the matrix **b** is expressed in Eq 12:

$$\begin{aligned} &\boldsymbol{b}(\theta) = \boldsymbol{a}(\theta)\boldsymbol{K} \\ &\boldsymbol{K} = [\boldsymbol{K_{tc}} \ \ \boldsymbol{K_{te}} \ \ \boldsymbol{K_{rc}} \ \ \boldsymbol{K_{re}} \ \ \boldsymbol{K_{ac}} \ \ \boldsymbol{K_{ae}}]^T; \\ &\boldsymbol{K_{pq}} = \begin{bmatrix} C_0^{pq} & C_1^{pq} & S_1^{pq} \end{bmatrix} \end{aligned} \quad (12)$$

The matrix $\boldsymbol{a}$ is of dimension 6 x [6 x (2M + 1)]. The matrix elements $\boldsymbol{a}$ can be found from the results of the integration of Eq. 9. These elements are provided in Appendix A for the slotting case.

The procedure for identifying the coefficients of the Fourier series of cutting coefficients is a two-step procedure.

4.1. Step 1

To create an over-determined system, it is necessary to carry out the tests with a number n of feed per tooth f_z values greater than two (n>2). To create the simplest model, n has been set to the minimum required (n=3). It is therefore possible to construct an over-determined system (Eq. 13):

$$\boldsymbol{F} = \boldsymbol{C}\boldsymbol{b}(\theta); \quad \boldsymbol{C} = \begin{bmatrix} \boldsymbol{c_1} \\ \boldsymbol{c_2} \\ \boldsymbol{c_3} \end{bmatrix}; \quad \boldsymbol{F} = \begin{bmatrix} \boldsymbol{f_1} \\ \boldsymbol{f_2} \\ \boldsymbol{f_3} \end{bmatrix} \quad (13)$$

where $\boldsymbol{c_1}$, $\boldsymbol{c_2}$, and $\boldsymbol{c_3}$ are the $\boldsymbol{c}$ matrices of Eq. 11 evaluated at the three feed per tooth values chosen; $\boldsymbol{f_1}$, $\boldsymbol{f_2}$, and $\boldsymbol{f_3}$ are the mean force vectors of Eq. 10 produced by the different feed per tooth. Two solutions were chosen to solve this system. The first is by using the Moore-Penrose pseudo-inverse directly on the $\boldsymbol{C}$ matrix (Eq. 14). The second (Eq. 15) is to apply this pseudo-inverse to a matrix $\mathbf{C}$ weighted by the matrix $\boldsymbol{W}$ (Eq. 16). This weighting matrix $\boldsymbol{W}$ is defined as the diagonal matrix containing the inverse of the square of the variance of the mean forces at each feed per tooth tested.

$$\boldsymbol{b}(\theta) = \boldsymbol{C}^{+}\boldsymbol{F} \quad with\ \boldsymbol{C}^{+} = (\boldsymbol{C}^{t}C)^{-1}\boldsymbol{C}^{t} \tag{14}$$

$$\boldsymbol{b}(\theta) = \boldsymbol{C}_{\boldsymbol{w}}^{+}\boldsymbol{F}_{\boldsymbol{w}}\ with\ \boldsymbol{C}_{\boldsymbol{w}} = \boldsymbol{W}\boldsymbol{C}, \boldsymbol{F}_{\boldsymbol{w}} = \boldsymbol{W}\boldsymbol{F} \tag{15}$$

$$\boldsymbol{W} = diag(1/\sigma_{x1}^2, 1/\sigma_{y1}^2, 1/\sigma_{x2}^2, 1/\sigma_{y2}^2, 1/\sigma_{x3}^2, 1/\sigma_{y3}^2) \tag{16}$$

4.2. Step 2

Step 1 is repeated for all m fiber orientation angles. m must be greater than ($2M$+1). To simplify the model, m has been set to this minimum value for M set to 1 (m=4). Thus, Eq. 12 can be written for each fiber orientation angle and expressed in matrix format (Eq. 17). This over-determined system (Eq. 17) is solved by the least squares method using the Moore-Penrose pseudo-inverse (Eq. 18).

$$B = A \cdot K; B = \begin{bmatrix} b(\theta_1) \\ \vdots \\ b(\theta_4) \end{bmatrix}; A = \begin{bmatrix} a(\theta_1) \\ \vdots \\ a(\theta_4) \end{bmatrix} \tag{17}$$

$$K = A^{+}B \tag{18}$$

5. Experimental setup

The experimental setup is shown in Fig. 2. The slotting tests were conducted on a Stäubli TX 200 robot with a Teknomotor ATC 71-HSK F63 spindle, from the UMONS Machine Design and Production Engineering Lab. A 6 mm diameter, 4-teeth milling cutter from Seco Tools, designed for machining thermoset or thermoplastic G/C-FRP, was used. The cutter has a 10° helix angle. The workpieces are UD-GFRP samples from Sobelcomp, consisting of 14 plies of unidirectional glass fibers with an epoxy matrix, all aligned in the same direction. The sample thickness is 7.3 mm ± 0.2 mm. Cutting forces were measured using a Kistler 9257B piezoelectric multicomponent dynamometer, with a sampling frequency of 40 kHz. The raw signal was low-pass filtered at 1800 Hz to eliminate high-frequency noise. The samples were clamped on the dynamometer. Table 1 summarizes the setup information.

The cutting conditions were chosen within Seco's recommendation range. The cutting speed Vc was set at 125 m/min. The axial depth of cut matches the sample thickness. A large sample thickness was chosen to limit sample flexibility and reduce noise in measurements. The identified coefficients will be used in models where only the peripheral teeth are considered. Consequently, machining is performed without the teeth to eliminate the contribution of the end teeth. To simplify the model, the Fourier series of the cutting coefficients was limited to the first order (M = 1), requiring at least four fiber orientations (m > 2M + 1). The chosen fiber orientation angles were 0, π/4, π/2, 3π/4. Additionally, three feed values per tooth were selected to fit Seco's operating range: 0.02, 0.03, and 0.04 mm/th. The cutting conditions are summarized in Table 2.

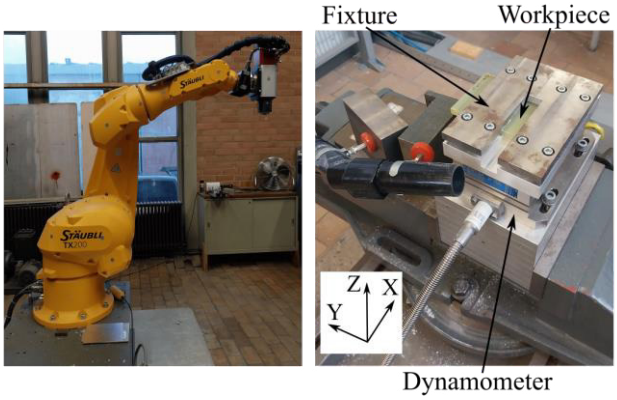

Fig. 2. Experimental setup.

Table 1. Setup information.

Property	Value
Machining robot	Stäubli TX 200
Tool	880060R020Z4.0-DURA
Number of teeth Z	4
Diameter of the tool D [mm]	6
Helix angle [deg]	10
Sample	UD-GFRP
Thickness t [mm]	7.3 ± 0.2
Dynamometer	9257B Kistler
Sampling frequency [kHz]	40

Table 2. Cutting conditions.

Property	Value
Axial depth of cut a_p [mm]	7.3
Radial depth of cut a_e [mm]	6
Cutting speed v_c [m/min]	125
Feed per tooth f_z [mm/th]	0.02 - 0.03 - 0.04
Orientation fiber angle θ [rad]	0 - π/4 - π/2 - 3π/4

Each slotting test was conducted over a length of 35 mm, but only a reduced interval equivalent to 100 rotations was used as input data to capture the steady-state portion of the machining. Tests with a machining robot are more subject to trajectory deviations compared to CNC tests. To overcome this problem, the tests were carried out in a workspace and posture that optimized the robot's rigidity. In addition, identification was carried out on the slotting operation to ensure that tool engagement angles (φ_{st} = 0, φ_{ext} = π) did not change despite deviations. However, using a machining robot helps evaluate the method's ability to identify cutting coefficients even under these conditions. Each cutting condition was repeated six times to address issues like fiber distribution, variable sample thickness, inclusions, and machining defects such as delamination and fiber pull-out.

6. Results

The method described in section 4 was applied to the data from the slotting operations using the setup detailed in section 5. The Fourier coefficients C_0, C_1, S_1 and C_{0w}, C_{1w}, S_{1w} for the different cutting coefficients K_{pq} (p = t, r, a; q = c, e) are summarized in Table 3. The Fourier coefficients C_{0w}, C_{1w}, S_{1w} were calculated from the expression of $\boldsymbol{b}$ in Eq. 15.

Table 3. Fourier coefficient of $K_{pq}(\beta)$.

Cutting coefficient	C_0	C_1	S_1	C_{0w}	C_{1w}	S_{1W}
$K_{tc}(\beta)$ [MPa]	255.9	15.8	18.4	255.7	7.6	16.4
$K_{rc}(\beta)$ [MPa]	358.8	-18.4	17.3	353.4	-16.4	7.6
$K_{ac}(\beta)$ [MPa]	48.2	-25.4	12	48	-30.7	6.6
$K_{te}(\beta)$ [N/mm]	6	-1	17.3	6.2	-1.2	11.1
$K_{re}(\beta)$ [N/mm]	1.5	11.5	1.4	1.6	7	2.1
$K_{ae}(\beta)$ [N/mm]	0.1	0	0	0.1	0	0

The shapes of the K_{pq} (Eq. 4) were plotted (Fig. 3) using the Fourier coefficients in Table 3. The contribution of the axial edge coefficient is almost zero. In addition, the tangential and radial edge coefficients have a negative part. This is a mathematical artefact that makes no physical sense.

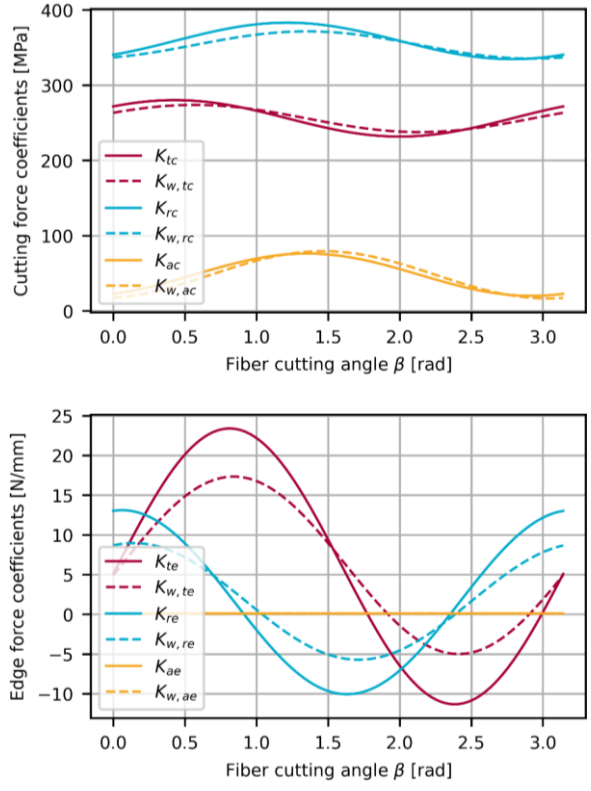

Fig. 3. Variable cutting and edge force coefficients identified.

Fig.4 shows the cutting forces (F_x, F_y and F_z) for the different values of θ tested for a feed per tooth f_z of 0.03 mm/th. The blue curve represents the measured forces, while the red and orange curves represent the forces modelled by Eq.15 and Eq.16 (with the weighting matrix) respectively.

The average forces of F_x, F_y and F_z coincide between the measurements and the modelling. However, it should be noted that the amplitude of the signal is mostly overestimated for F_x and F_y. The amplitude is underestimated for F_z. The lack of rigidity in robots compared to traditional CNC machines justifies this. Additionally, axial forces F_z are typically less significant and not prioritized over in-plane forces F_x and F_y, an assumption that doesn't hold in robotic machining. Furthermore, the measured forces may not be periodic throughout the entire period, likely due to the dynamic effects of robotic machining. The forces calculated using the weighting matrix (Eq. 16) are more consistent with the measurements.

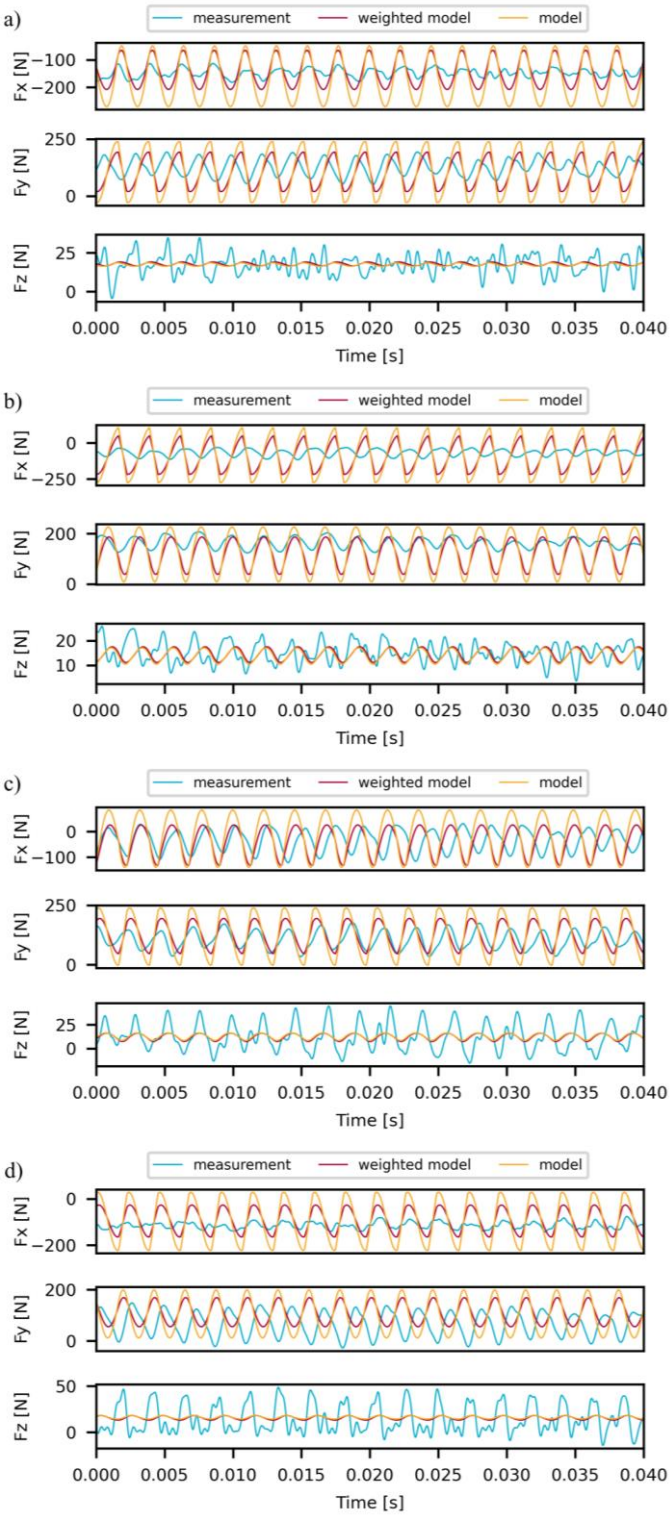

Fig. 4. Cutting forces for (a) $\theta = 0$, (b) $\theta = \pi/4$, (c) $\theta = \pi/2$, (d) $\theta = 3\pi/4$

Thus, cutting forces can also be modelled for shoulder milling (50% immersion in up milling). Fig. 5 displays the measured and modelled forces (using the weighting matrix). In general, the modelling of forces F_x and F_y is satisfactory in terms of mean value and amplitude. However, while the average level of forces F_z is correct, the amplitude is significantly underestimated. The objective of accurately modelling the average cutting forces has been achieved, but the modelling of effort amplitudes still needs improvement.

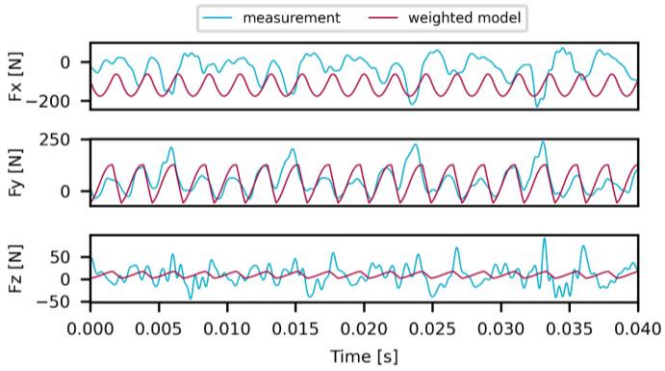

Fig. 5. Cutting forces in shoulder milling for $\theta = 0$, $f_z = 0.03$ mm/th.

7. Conclusion

A mechanistic model has been developed to calculate cutting forces in all three spatial directions during the machining of unidirectional glass fiber-reinforced polymers (UD-GFRP). This model incorporates the adjustment of cutting coefficients based on the instantaneous fiber cutting angle, capturing variations in the chip formation process. The cutting coefficients are modeled as periodic functions to reflect the cyclical nature of the cutting phenomena associated with fiber orientation. The chosen function is a first-order Fourier series.

The model's validity was established through experimental validation in robotically milled UD-GFRP. First, the accuracy of the identification method was assessed using slotting experiments, providing a baseline for calibration. The slotting operation was chosen because, despite deviations due to low robot rigidity, the tool engagement angles remain unchanged. Second, the model's performance was demonstrated by predicting cutting forces during shoulder milling (50% immersion in up milling). The objective of accurately modeling the average level of cutting forces has been achieved, but the modeling of effort amplitudes still requires improvement.

This approach enables the straightforward calibration of a mechanistic model by utilizing milling force data to adjust the model parameters. However, the current version of the model does not account for factors such as tool wear, fiber pull-out, or delamination, which may influence the cutting forces and the quality of the finished part. Future work will focus on extending the model's applicability to multidirectional glass fiber-reinforced polymers (MD-GFRP), with the aim of further validating and refining the model to better reflect the complex behaviors observed in these composite materials. Using a 2nd-order Fourier series could be a potential solution, even if it removes some of the physical meaning from the model.

Acknowledgements

The authors would like to thank Région Wallonne for supporting this research as part of the MachFlexComp M-ERA.NET 2022 research project under grant 2210138.

Appendix A. Matrix *a(θ)*

The non-zero entries of the matrix $a(\theta)$ of Eq. 12 are shown in Table 4 for the slotting case ($\varphi_{st} = 0$, $\varphi_{ext} = \pi$). with N the number of teeth, a_p the axial depth of cut and θ the fiber orientation angle.

Table 4. Non-zero entries of the 6x18 matrix $a(\theta)$.

Value	
$a_{1,2} = a_{1,9} = a_{3,8} = Z\,a_p \sin(2\theta)/\,8$	$a_{2,10} = -a_{4,4} = -a_{5,13} = -Z\,a_p/\pi$
$a_{1,3} = a_{3,2} = a_{3,9} = -Z\,a_p \cos(2\theta)\,/8$	$a_{2,11} = Z\,a_p \cos(2\theta)\,/(3\pi)$
$a_{1,7} = -a_{3,1} = -a_{6,16} = -Z\,a_p/4$	$a_{2,12} = Z\,a_p \sin(2\theta)\,/(3\pi)$
$a_{1,8} = Z\,a_p \cos(2\theta)\,/8$	$a_{3,3} = -Z\,a_p \sin(2\theta)\,/8$
$a_{2,5} = a_{4,11} = 2\,Z\,a_p \sin(2\theta)\,/(3\pi)$	$a_{4,5} = a_{5,14} = -Z\,a_p \cos(2\theta)\,/(3\pi)$
$a_{2,6} = a_{4,12} = -2\,Z\,a_p \cos(2\theta)\,/(3\pi)$	$a_{4,6} = a_{5,15} = -Z\,a_p \sin(2\theta)\,/(3\pi)$

References

[1] Y. Song, H. Cao, W. Zheng, D. Qu, L. Liu, and C. Yan, 'Cutting force modeling of machining carbon fiber reinforced polymer (CFRP) composites: A review', *Compos. Struct.*, vol. 299, p. 116096, Nov. 2022.

[2] G. V. G. Rao, P. Mahajan, and N. Bhatnagar, 'Micro-mechanical modeling of machining of FRP composites – Cutting force analysis', *Compos. Sci. Technol.*, vol. 67, no. 3–4, pp. 579–593, Mar. 2007.

[3] R. Rentsch, O. Pecat, and E. Brinksmeier, 'Macro and micro process modeling of the cutting of carbon fiber reinforced plastics using FEM', *Procedia Eng.*, vol. 10, pp. 1823–1828, Jan. 2011.

[4] D. Iliescu, D. Gehin, I. Iordanoff, F. Girot, and M. E. Gutiérrez, 'A discrete element method for the simulation of CFRP cutting', *Compos. Sci. Technol.*, vol. 70, no. 1, pp. 73–80, Jan. 2010.

[5] R. Mullin, M. Farhadmanesh, A. Ahmadian, and K. Ahmadi, 'Modeling and identification of cutting forces in milling of Carbon Fibre Reinforced Polymers', *J. Mater. Process. Technol.*, vol. 280, p. 116595, Jun. 2020.

[6] Y. Karpat, O. Bahtiyar, and B. Değer, 'Mechanistic force modeling for milling of unidirectional carbon fiber reinforced polymer laminates', *Int. J. Mach. Tools Manuf.*, vol. 56, pp. 79–93, May 2012.

[7] J. Ahmad, *Machining of Polymer Composites*. Boston, MA: Springer US, 2009.

[8] Y. He, J. Sheikh-Ahmad, S. Zhu, and C. Zhao, 'Cutting force analysis considering edge effects in the milling of carbon fiber reinforced polymer composite', *J. Mater. Process. Technol.*, vol. 279, p. 116541, May 2020.

[9] H. Cao, Y. Song, B. Wu, K. Wang, and D. Qu, 'A force model of high-speed dry milling CF/PEEK considering fiber distribution characteristics', *J. Manuf. Process.*, vol. 68, pp. 602–615, Aug. 2021.

[10] J. Mei, O. G. Diaz, and D. A. Axinte, 'Modelling the unidirectional fibre composite milling force oscillations through capturing the influence of the stochastic fibre distributions', *Compos. Struct.*, vol. 226, p. 111188, Oct. 2019.

[11] Y. Altintas, *Manufacturing Automation: Metal Cutting Mechanics, Machine Tool Vibrations, and CNC Design*. Cambridge University Press, 2000.

[12] 'JC880/885 - Fraise 2 tailles - Composite - 4 dents | Secotools.com'. Accessed: Nov. 25, 2024. [Online]. Available: https://www.secotools.com/article/m_7560

[13] Y. Altintaş and P. Lee, 'A General Mechanics and Dynamics Model for Helical End Mills', *CIRP Ann.*, vol. 45, no. 1, pp. 59–64, Jan. 1996.